PROCEEDINGS B

royalsocietypublishing.org/journal/rspb

Research

Cite this article: Seymour RS, Bosiocic V, Snelling EP, Chikezie PC, Hu Q, Nelson TJ, Zipfel B, Miller CV. 2019 Cerebral blood flow rates in recent great apes are greater than in *Australopithecus* species that had equal or larger brains. *Proc. R. Soc. B* **286**: 20192208. http://dx.doi.org/10.1098/rspb.2019.2208

Received: 22 September 2019
Accepted: 21 October 2019

Subject Category:
Palaeobiology

Subject Areas:
cognition, evolution, physiology

Keywords:
brain, cognition, evolution, hominin, perfusion, primate

Author for correspondence:
Roger S. Seymour
e-mail: roger.seymour@adelaide.edu.au

Electronic supplementary material is available online at https://dx.doi.org/10.6084/m9.figshare.c.4714553.

THE ROYAL SOCIETY PUBLISHING

Cerebral blood flow rates in recent great apes are greater than in *Australopithecus* species that had equal or larger brains

Roger S. Seymour[1], Vanya Bosiocic[1], Edward P. Snelling[2,3], Prince C. Chikezie[3], Qiaohui Hu[1], Thomas J. Nelson[1], Bernhard Zipfel[4] and Case V. Miller[5]

[1]School of Biological Sciences, Faculty of Sciences, University of Adelaide, Adelaide, South Australia 5005, Australia
[2]Department of Anatomy and Physiology, Faculty of Veterinary Science, University of Pretoria, Onderstepoort 0110, South Africa
[3]Brain Function Research Group, School of Physiology, and [4]Evolutionary Studies Institute, University of the Witwatersrand, Johannesburg 2193, South Africa
[5]Vertebrate Palaeontology Laboratory, Department of Earth Sciences, University of Hong Kong, Pok Fu Lam, Hong Kong

RSS, 0000-0002-3395-0059; EPS, 0000-0002-8985-8737; PCC, 0000-0002-3004-1896; QH, 0000-0003-3163-7859; TJN, 0000-0002-7209-2915; BZ, 0000-0002-4251-884X; CVM, 0000-0002-6467-0199

Brain metabolic rate (MR) is linked mainly to the cost of synaptic activity, so may be a better correlate of cognitive ability than brain size alone. Among primates, the sizes of arterial foramina in recent and fossil skulls can be used to evaluate brain blood flow rate, which is proportional to brain MR. We use this approach to calculate flow rate in the internal carotid arteries ($\dot{Q}_{ICA}$), which supply most of the primate cerebrum. $\dot{Q}_{ICA}$ is up to two times higher in recent gorillas, chimpanzees and orangutans compared with 3-million-year-old australopithecine human relatives, which had equal or larger brains. The scaling relationships between $\dot{Q}_{ICA}$ and brain volume (V_{br}) show exponents of 1.03 across 44 species of living haplorhine primates and 1.41 across 12 species of fossil hominins. Thus, the evolutionary trajectory for brain perfusion is much steeper among ancestral hominins than would be predicted from living primates. Between 4.4-million-year-old *Ardipithecus* and *Homo sapiens*, V_{br} increased 4.7-fold, but $\dot{Q}_{ICA}$ increased 9.3-fold, indicating an approximate doubling of metabolic intensity of brain tissue. By contrast, $\dot{Q}_{ICA}$ is proportional to V_{br} among haplorhine primates, suggesting a constant volume-specific brain MR.

1. Introduction

Brain size is the usual measure in discussions of the evolution of cognitive ability among primates, despite recognized shortcomings [1]. Although absolute brain size appears to correlate better with cognitive ability than encephalization quotient, progression index or neocortex ratio [2,3], an even better correlate might be brain metabolic rate (MR), because it represents the energy cost of neurological function. However, brain MR is difficult to measure directly in living primates and impossible in extinct ones.

One solution to the problem has been to measure oxygen consumption rates and glucose uptake rates on living mammals in relation to brain size and then apply the results to brain sizes of living and extinct primates. Because physiological rates rarely relate linearly to volumes or masses of tissues, any comparison requires allometric analysis. For example, brain MR can be analysed in relation to endocranial volume (≈ brain volume, V_{br}) with an allometric equation of the form, $MR = aV_{br}^{b}$, where a is the elevation (or scaling factor, indicating the height of the curve) and b is the scaling exponent (indicating the shape of the curve on arithmetic axes). If $b = 1.0$, then MR is directly

proportional to brain size. If b is less than 1, then MR increases with brain size, but the metabolic intensity per unit volume of neural tissue decreases. If b is greater than 1, the metabolic intensity of neural tissue increases. The exponent for brain MR measured as oxygen consumption and glucose use across several mammalian species is approximately 0.86, and the exponent for cortical brain blood flow rate in mammals is between 0.81 and 0.87 [4,5]. The similarity of the exponents indicates that blood flow rate is a good proxy for brain MR in mammals in general. The exponents are less than 1.0, which shows that brain MR and blood flow rate increase with brain size but with decreasing metabolic and perfusion intensities of the neural tissue.

Recent studies show that blood flow rate in the internal carotid artery ($\dot{Q}_{ICA}$) can be calculated from the size of the carotid foramen through which it passes to the brain [6]. The artery occupies the foramen lumen almost entirely [7–9], therefore defining the outer radius of the artery (r_o), from which inner lumen radius (r_i) can be estimated, assuming that arterial wall thickness ($r_o - r_i$) is a constant ratio (w) with lumen radius ($w = (r_o - r_i)/r_i$), according to the law of Laplace. The haemodynamic equation used to calculate $\dot{Q}_{ICA}$ is referred to as the 'shear stress equation', and attributed to Poiseuille: $\dot{Q} = (\tau\pi r_i^3)/(4\eta)$, where $\dot{Q}$ is the blood flow rate ($cm^3\ s^{-1}$), τ is the wall shear stress ($dyn\ cm^{-2}$), r_i is the arterial lumen radius (cm) and η is the blood viscosity ($dyn\ s\ cm^{-2}$) [10]. The technique was validated in mice, rats and humans, but was initially criticized [11], defended [12] and subsequently accepted [13]. However, the calculations involved three questionable assumptions: flow in the cephalic arteries conforms to Poiseuille flow theory, arterial wall shear stress can be calculated accurately from body mass (although there is no clear functional relationship between them) and the arterial wall thickness-to-lumen radius ratio (w) was a certain constant derived from only two values in the literature.

We have now made significant advancements to the initial methodology by replacing the shear stress equation, and its assumptions, with a new equation derived empirically from a meta-analysis of $\dot{Q}$ versus r_i in 30 studies of seven cephalic arteries of six mammalian genera, arriving at an allometric, so-called 'empirical equation', $\dot{Q} = 155\ r_i^{2.49}$ ($R^2 = 0.94$) [14]. The equation is based on stable cephalic flow rates, which vary little between rest, intense physical activity, mental exercise or sleep [14]. The equation also eliminates reliance on the somewhat tenuous estimation of arterial wall shear stress from body mass. We have also improved the calculation with a more extensive re-evaluation of carotid arterial wall thickness ratio ($w = 0.30$) from 14 imaging studies on humans (electronic supplementary material, text and table S1 for data and references). The present investigation implements these recent methodological advancements and re-evaluates the scaling of $\dot{Q}_{ICA}$ as a function of V_{br} in extant haplorhine primates and in fossil hominins. The point of our study is to clarify these relationships between *Homo sapiens*, *Australopithecus* and modern great apes (*Pongo*, *Pan*, *Gorilla*) to resolve an apparent allometric conundrum within our previous studies: one analysis based on 34 species of extant Haplorhini, including *H. sapiens*, resulted in the equation $\dot{Q}_{ICA} = 8.82 \times 10^{-3}\ V_{br}^{0.95}$ [6], while another analysis of 11 species of fossil hominin, also including *H. sapiens*, produced the equation $\dot{Q}_{ICA} = 1.70 \times 10^{-4}\ V_{br}^{1.45}$ [15]. Humans are on both analyses with the largest brains, but the exponents of these equations are markedly different, and the lines converge. The present study confirms that hominin ancestors had lower $\dot{Q}_{ICA}$ than predicted from V_{br} with the haplorhine equation. $\dot{Q}_{ICA}$ in modern great apes is about twice that in *Australopithecus* species, despite similar or smaller V_{br}.

2. Results

(a) Internal carotid artery blood flow rate in extant great apes and *Australopithecus*

Because two internal carotid arteries (ICAs) enter the brain, all reported values of $\dot{Q}_{ICA}$ are the sum of flows in the right and left ICAs derived from individual foramina or twice the value calculated from one intact foramen in fossil skulls. $\dot{Q}_{ICA}$ in relation to V_{br} in recent *Pongo*, *Pan*, *Gorilla* and *Homo* and in fossil *Australopithecus* reveal significant differences (figure 1; see electronic supplementary material, table S2 for individual species data). ANOVA and Tukey's multiple comparisons test distinguish all five genera from one another, except between *Pongo* and *Pan* (table 1). $\dot{Q}_{ICA}$ in *Australopithecus* was the lowest of all genera and it sits very far below the 95% confidence belt, and below the 95% prediction limits for a linear regression of $\log_{10}\ \dot{Q}_{ICA}$ on $\log_{10}\ V_{br}$ for the living genera (figure 1 inset). The prediction limits are a statistically rigorous way of testing whether a single point is significantly different from a group [16]. Thus, $\dot{Q}_{ICA}$ is significantly higher in all genera of modern great apes compared to *Australopithecus* despite equal or smaller V_{br}.

(b) Internal carotid artery blood flow rate in fossil hominins and extant haplorhine primates

Carotid foramen radius (r_o, cm) and endocranial brain volume (V_{br}, ml) in fossil hominin skulls, including *Ardipithecus ramidus*, produce the regression $r_o = 0.0048\ V_{br}^{0.57\pm0.12\ CI}$ ($R^2 = 0.91$). New values of $\dot{Q}_{ICA}$ calculated with the empirical equation and $w = 0.30$ in 44 species of extant haplorhine primates and 12 species of fossil hominins are compared in figure 2 (see electronic supplementary material, table S3 for individual species data). The new regressions are $\dot{Q}_{ICA} = 0.0068\ V_{br}^{1.03\pm0.07\ CI}$ ($R^2 = 0.95$) for haplorhines and $\dot{Q}_{ICA} = 0.00028\ V_{br}^{1.41\pm0.30\ CI}$ ($R^2 = 0.91$) for hominins. The two exponents are significantly different ($F_{1,53} = 6.27$; $p = 0.015$), and there is no overlap of data between the two groups (Johnson–Neyman test revealed significant differences in the $\dot{Q}_{ICA}$ data below $V_{br} = 1708$ ml, which exceeds all data). The exponent for haplorhines is not significantly different from 1.0, meaning that $\dot{Q}_{ICA}$ is directly proportional to V_{br}. By contrast, the extremely high exponent for hominins shows that V_{br} increased 4.7-fold, whereas $\dot{Q}_{ICA}$ increased 9.3-fold, between *Ardipithecus* and *H. sapiens*, revealing an approximately twofold increase in volume-specific perfusion rate of the neural tissue across hominin evolution.

Recent analyses of primate regional brain anatomy, including the volumes of neocortical grey matter (V_{grey}) and telencephalon (V_{tele}), are now available [17–19] (electronic supplementary material, table S4). These data include 17 species of extant haplorhine primates for which we have ICA foramen radius [6,13]. Assuming $w = 0.30$ and using the empirical equation, we find $\dot{Q}_{ICA} = 0.0135\ V_{grey}^{1.06\pm0.14\ CI}$

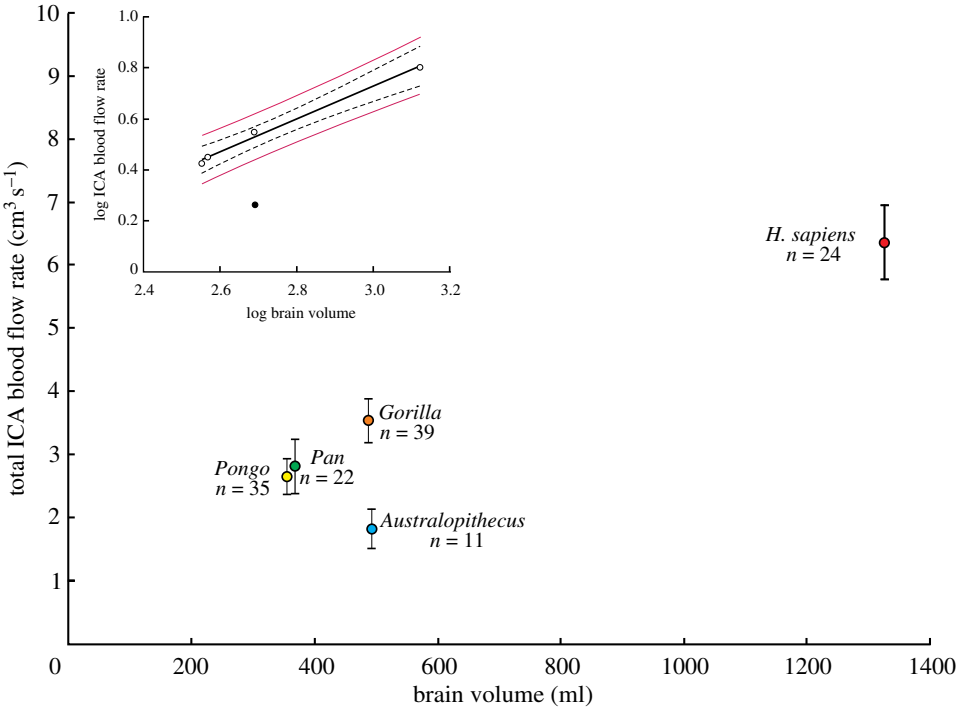

Figure 1. Total blood flow rate of both ICAs ($\dot{Q}_{ICA}$), calculated from ICA foramen radius data with the new, 'empirical equation' and a wall thickness-to-lumen radius ratio of $w = 0.30$, in relation to brain volume (V_{br}) in selected hominids. Means, 95% CI and sample sizes are shown. Inset is the regression of $\log_{10} \dot{Q}_{ICA}$ against $\log_{10} V_{br}$ for four genera of hominids, namely *Pongo*, *Pan*, *Gorilla* and archaic *H. sapiens* (unfilled circles), showing that *Australopithecus* (filled circle) falls well below the regression mean's 95% confidence bands (dashed lines) and 95% prediction limits (thin red lines). See electronic supplementary material, table S2 for statistics of individual species. (Online version in colour.)

Table 1. Results of ANOVA ($F_{4,126} = 43$, $p < 0.0001$) and Tukey's post hoc test comparing differences in total blood flow rate of both internal carotid arteries ($\dot{Q}_{ICA}$) in four genera of hominids. *p*-values less than or equal to 0.05 indicate a statistically significant difference.

	Pongo	*Pan*	*Homo*	*Australopithecus*
Gorilla	0.0012	0.036	<0.0001	<0.0001
Pongo		0.98 (n.s.)	<0.0001	0.0123
Pan			<0.0001	0.0066
Homo				<0.0001

($R^2 = 0.95$) (figure 3*a*) and $\dot{Q}_{ICA} = 0.0103\ V_{tele}^{1.01\pm0.12\ CI}$ ($R^2 = 0.96$) (figure 3*b*). Both exponents are not significantly different from 1.0. We also have ICA foramen sizes for 26 species of haplorhine primates and 15 species of strepsirrhine primates in which total volume of the neocortex (V_{neo}), including white and grey matter, has been measured [20,21] (electronic supplementary material, table S5). The regressions for these species are $\dot{Q}_{ICA} = 0.0062\ V_{neo}^{1.12\pm0.15\ CI}$ ($R^2 = 0.91$) for haplorhines and $\dot{Q}_{ICA} = 0.0012\ V_{neo}^{0.96\pm0.42\ CI}$ ($R^2 = 0.66$) for strepsirrhines (electronic supplementary material, figure S1). The regression for strepsirrhines is not particularly tight, so the exponent is not significantly different from the haplorhines ($F_{1,37} = 0.692$; $p = 0.41$), but the elevation is significantly lower in strepsirrhines ($F_{1,38} = 74.18$; $p < 0.0001$). Strepsirrhine primates have reduced ICA and a different pattern of brain perfusion [22], which explains low $\dot{Q}_{ICA}$ found in this and previous studies [6]. Therefore, we consider only haplorhines, in which only the internal carotid and vertebral arteries supply the brain. The scaling of ICA blood flow rate in haplorhine primates in relation to different measures of total or partial brain volumes show exponents not significantly different from 1.0, but significantly higher than 0.86, the exponent apparent in mammals in general [4,5].

3. Discussion

The major point of this paper is a comparison of blood flow rate in the internal carotid arteries ($\dot{Q}_{ICA}$) of recent great apes and extinct species of *Australopithecus*, as assessed with a new, empirical method from the size of the carotid foramina in the skull. It was unexpected to find that $\dot{Q}_{ICA}$ was significantly higher in recent great apes (figure 1), because the ICAs are the major blood supply to the cerebral cortex, and the cognitive ability of *Australopithecus* is considered superior to that of great apes [23,24]. To understand the basis of this finding, §3(a) considers the sources of brain blood flow and how they relate to brain volume among extant haplorhine primates, including the roles of the ICAs and the vertebral arteries (VAs). Next, §3(b) follows with the implications of the great difference between the scaling of $\dot{Q}_{ICA}$ with brain volume between extant haplorhines and extinct hominins, including the role of the VAs in total brain perfusion. Finally, §3(c) discusses the connection between brain perfusion, brain MR and cognitive ability in great apes and *Australopithecus*.

(a) Brain perfusion in extant haplorhine primates

The entire brain of haplorhine primates is supplied by two paired arteries, the ICAs and VAs. These arteries communicate with each other in the circle of Willis (cerebral arterial circle) through the paired posterior communicating arteries. In humans, the ICAs supply all of the anterior and middle

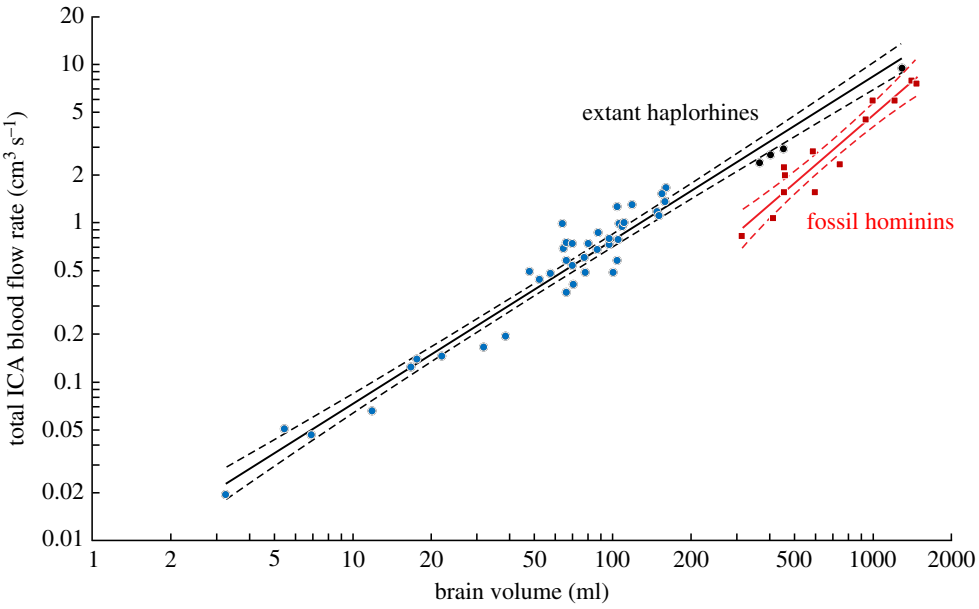

Figure 2. Total blood flow rate of both ICAs ($\dot{Q}_{ICA}$) in relation to brain volume (V_{br}). $\dot{Q}_{ICA}$ is calculated from ICA foramen radius data with a wall thickness-to-lumen radius ratio (w) of 0.30 and the new empirical equation. The regression equation for 44 species of extant haplorhine primates (blue and black circles) is $\dot{Q}_{ICA} = 0.0068\ V_{br}^{1.03\pm0.07\ CI}$ ($R^2 = 0.95$), and that for 12 species of fossil hominins (red squares) is $\dot{Q}_{ICA} = 0.00028\ V_{br}^{1.41\pm0.30\ CI}$ ($R^2 = 0.91$). Solid lines are the regression means; dashed lines are 95% confidence bands. Black circles are *Pongo*, *Pan*, *Gorilla* and *H. sapiens*. See electronic supplementary material, table S3 for data derived from [6,13,15]. (Online version in colour.)

cerebral arteries, while the VAs supply mainly the arteries of the upper spinal cord, brainstem and cerebellum. Supply to the posterior cerebral arteries is shared. A meta-analysis of 19 studies of normal human cephalic circulation shows that the sum of the flow rates in three paired cerebral arteries is 9.2 cm^3 s^{-1} and the sum of the flow rates in both ICAs is 8.1 cm^3 s^{-1} [25]. Thus, the ICAs account for 88%, and the VAs account for 12%, of total cerebral perfusion.

Although the ICAs supply approximately 75%, and the VAs 25%, of total brain perfusion ($\dot{Q}_{TOTAL}$) in humans [25–31], these proportions approach each other in extant haplorhine species with smaller brains until they become approximately equal in brains smaller than 10 ml. (See the electronic supplementary material, including figure S5, for a detailed analysis of the roles of the VAs and ICAs in extant haplorhines.) Allometrically, these relationships manifest as divergent exponents: $\dot{Q}_{ICA} = 0.0065\ V_{br}^{1.01}$, $\dot{Q}_{VA} = 0.0083\ V_{br}^{0.84}$ and $\dot{Q}_{TOTAL} = 0.0143\ V_{br}^{0.95}$. Thus the scaling of $\dot{Q}_{ICA}$ against V_{br} is isometric (directly proportional), but the scaling of $\dot{Q}_{VA}$ against V_{br} is hypoallometric (less than proportional). Not only is the $\dot{Q}_{ICA}$ exponent in haplorhines near 1.0 in relation to brain volume (figure 2), it is also near 1.0 in relation to neocortical grey matter volume (figure 3*a*), telencephalon volume (figure 3*b*) and neocortex volume (electronic supplementary material, figure S1). The exponents are all statistically significantly higher than 0.86 expected for total brain perfusion in mammals in general [4,5]. The difference between exponents of 1.0 and 0.86 is not trivial. Over the range of V_{br} of the haplorhines, volume-specific $\dot{Q}_{ICA}$ does not change at all with an exponent of 1.0, but drops to 50% with an exponent of 0.86.

The neocortex appears to be a constant fraction of total brain volume in primates, but the degree of superficial folding (gyrification) of the cortical surface area increases disproportionately [32,33]. Increased cortical surface area has been linked to intelligence [34]. Haplorhine $\dot{Q}_{ICA}$ increases in proportion to neocortical grey matter volume (figure 3*a*), telencephalon volume (figure 3*b*) and neocortex volume (electronic supplementary material, figure S1). Most of the volume increase in the cerebral cortex is due to an increase in the communication network (white matter) rather than the cognitive tissue, rich in synapses (grey matter). In haplorhine primates, the volume of grey matter increases with total brain volume to the 0.985 power (nearly linearly proportional), but white matter increases with the 1.241 power [33]. Our analysis shows that $\dot{Q}_{ICA}$ scales with $V_{br}^{1.03}$ (figure 2), corresponding well to the scaling of neocortical grey matter but not white matter. This seems reasonable because grey matter has an approximately 80-fold higher density of synapses [35], fourfold greater volume-specific energy use [36] and two to four times greater volume-specific perfusion rate than white matter [37,38]. Thus, grey matter may have a greater influence on the scaling of $\dot{Q}_{ICA}$ against V_{br} than white matter. Because cognition is largely associated with synapses in grey matter, it follows that blood flow rate is related to cognition.

Because both body mass and V_{br} tended to increase during primate evolution, and because $\dot{Q}_{ICA}$ is proportional to V_{br}, the allometry of $\dot{Q}_{ICA}$ and V_{br} in living species (figure 2) may roughly reflect their evolutionary history. The Haplorhini split from the Strepsirrhini around 66–69 Ma; within the Haplorhini, the Platyrrhini (New World monkeys) split from the Catarrhini (Old World monkeys and apes) around 46 Ma; within the Catarrhini, the Hominoidea (apes) arose around 32 Ma and the Hylobatidae (lesser apes and gibbons) split from the Hominidae (great apes) around 19 Ma [39]. Thus, the smaller-brained platyrrhines tend to have the oldest lineages, and larger-brained hominids represent the youngest. The progression of increasing perfusion correlates with the evolutionary order of 'information processing capacity' among haplorhines as indicated not only from anatomy and physiology (e.g. number of neurons, degree of connectivity, axonal conduction velocity), but also from behavioural measures (e.g. capacity

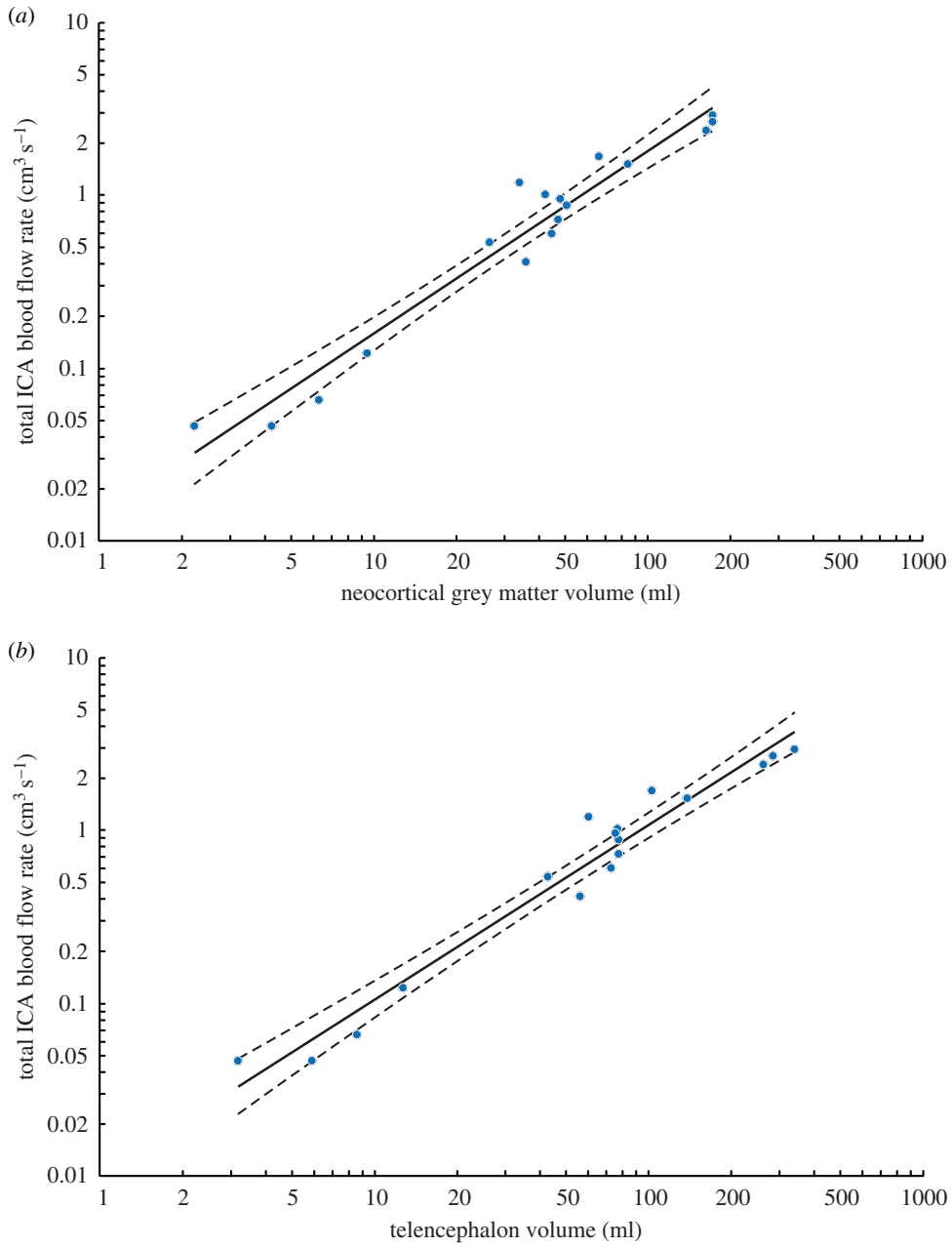

Figure 3. Total blood flow rate of both ICAs ($\dot{Q}_{ICA}$) in relation to (*a*) neocortical grey matter volume (V_{grey}) and (*b*) telencephalon volume (V_{tele}) in 17 species of extant haplorhine primates. $\dot{Q}_{ICA}$ values calculated with the new empirical equation and $w = 0.30$ from ICA foramen radii in [6,13]. Volume data are from [17], which include data from [18,19]; duplicate or triplicate data were averaged to obtain one point for each species. The equations are, $\dot{Q}_{ICA} = 0.0135\ V_{grey}^{1.06\pm0.14\ CI}$ ($R^2 = 0.95$) and $\dot{Q}_{ICA} = 0.0103\ V_{tele}^{1.01\pm0.12\ CI}$ ($R^2 = 0.96$). Solid line is the regression mean; dashed lines represent the 95% confidence bands. See electronic supplementary material, table S4 for individual data. (Online version in colour.)

for memory, mental manipulation, social interactions) [24,40]. Unfortunately, we have no data on ICA foramen size from fossil non-hominin haplorhines to test this idea.

(b) Internal carotid artery blood flow rate in extant great apes and *Australopithecus*

The present study indicates that the extant non-human great apes have a significantly greater absolute cerebral blood flow, and by inference metabolic demand, than ancestral *Australopithecus* (figure 1). Although *Gorilla* has V_{br} values similar to *Australopithecus*, *Gorilla* $\dot{Q}_{ICA}$ is approximately twice as high. *Pongo* and *Pan* have smaller V_{br} than *Australopithecus*, but significantly higher $\dot{Q}_{ICA}$. The difference is also apparent in $\dot{Q}_{ICA}$ scaling of extant haplorhine primates and fossil hominins from the literature (figure 2), where the great apes (black points) are higher than those for hominins. The implication of these disparate results is that the human brain appears to be a proportionately scaled up (nearly isometric exponent of 1.03) version of a recent haplorhine primate brain, something noted previously [41–43], but the allometry of $\dot{Q}_{ICA}$ in relation to V_{br} among the fossil hominins is very much steeper (hyperallometric exponent of 1.41).

The hominin exponent is similar to 1.45 calculated formerly from the shear stress equation [15]. The major determinate of $\dot{Q}_{ICA}$ is the extremely high allometric exponent of ICA foramen radius, which scales with $V_{br}^{0.57}$. If the skull increased in size while maintaining the same shape (isometric scaling), ICA radius would scale with $V_{br}^{0.33}$. If brain perfusion is assumed to scale with hypoallometry (e.g. $V_{br}^{0.86}$), then foramen radius would scale with an exponent even less than 0.33. Therefore, the high exponent for hominin ICA foramen radius

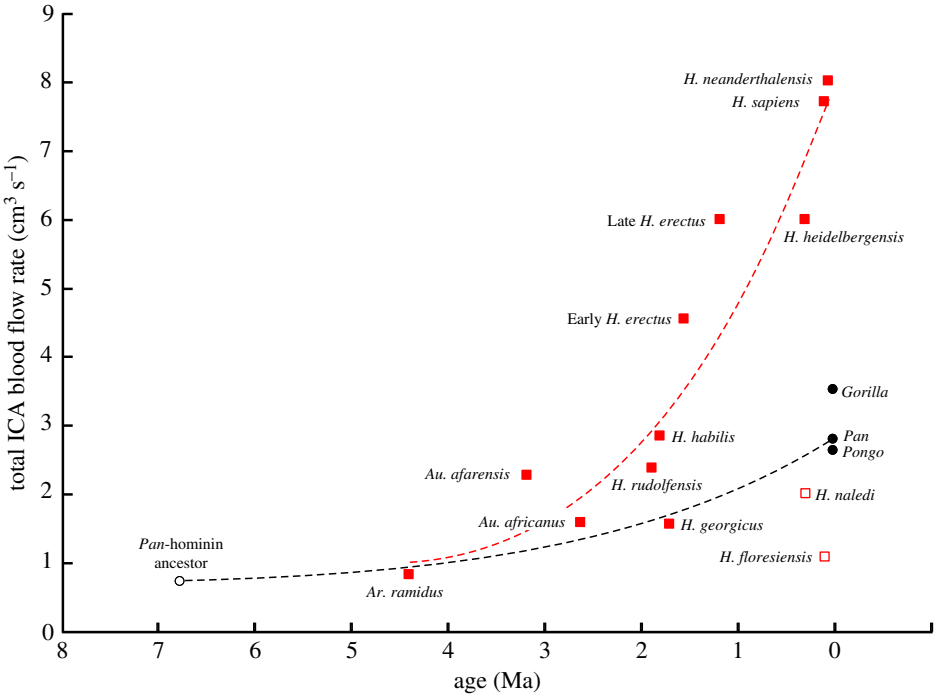

Figure 4. Total blood flow rate of both ICAs $(\dot{Q}_{ICA})$ in relation to age of hominins (red squares) and recent great apes (black circles). Two unusual hominin species (open squares) are *Homo naledi* and *Homo floresiensis*, which are excluded from the third-order polynomial curve used to visualize hominin evolution. A hypothetical common ancestor of *Pan–Homo sapiens* lineages is proposed at 6.75 Ma [39,45,46] with $\dot{Q}_{ICA}$ similar to that of *A. ramidus*. The evolutionary trajectories from this ancestor are both upward, but of different magnitudes. (Online version in colour.)

can mean nothing but an extraordinary increase in brain perfusion by the ICAs.

Although the ICAs appear to be associated with the cerebral cortex and cognition, it is reasonable to ask whether the VAs could have supplied significant blood to the cerebral cortex of *Australopithecus* to compensate for a hypothetically low ICA component. Assuming that the 500 ml brain of *Australopithecus* conformed to the pattern set by extant haplorhines, the ICAs would contribute 69%, and the VAs 31%, of total perfusion (see the equations in §3(a) of the discussion and electronic supplementary material, figure S5). So even if $\dot{Q}_{VA} = 0.82\,cm^3\,s^{-1}$ were added to the mean of $\dot{Q}_{ICA} = 1.84\,cm^3\,s^{-1}$ for *Australopithecus*, the total $2.66\,cm^3\,s^{-1}$ would still be less than $\dot{Q}_{ICA} = 3.54\,cm^3\,s^{-1}$ in the gorilla's ICAs alone, without any flow from its VAs (figure 1). It has been estimated from the carotid and transverse foramina of *Gorilla* that $\dot{Q}_{VA}$ may be higher than $\dot{Q}_{ICA}$ [13]. Therefore, *Australopithecus* cannot reach the level of total brain perfusion in *Gorilla* with scaling derived from extant haplorhine primates.

Moreover, it is difficult to reconcile the extremely high exponent for $\dot{Q}_{ICA}$ in hominins (1.41) with any expected scaling of $\dot{Q}_{TOTAL}$. Assuming an isometric exponent for $\dot{Q}_{TOTAL}$ (1.0), the exponent for $\dot{Q}_{VA}$ would need to be very much lower, approximately 0.36. (See the electronic supplementary material, including figure S6, for a model of the roles of the VAs and ICAs in hominins.) Under these assumptions, the 500 ml brain of *Australopithecus* would receive 47% of the blood from the ICAs and 53% from the VAs. Such a scenario would require the size of the VAs to decrease relative to the size of the brain during the evolution from *Australopithecus* to *H. sapiens*. This is possible, but cannot be easily tested, because, unlike the carotid foramen that contains the ICA and little else, the transverse foramen on the cervical vertebra passes not only the VA but also a large venous plexus [12]. If a cervical vertebra from *Australopithecus* could be analysed with certain assumptions [13], however, it may shed light on this question. For now, we hypothesize that the high scaling of $\dot{Q}_{ICA}$ is more likely to be associated with rapid increase in cortical MR during hominin evolution than a greater role of the VAs in *Australopithecus*.

(c) Implications of internal carotid artery brain perfusion

The results cast doubt over the notion that the neurological and cognitive traits of recent great apes adequately represent the abilities of *Australopithecus* species. The use of modern primates as a proxy for hominin evolution may have prevailed historically due to similar brain sizes, with the great apes between 300 and 500 ml, compared with 315 ml in *Ardipithecus* [44] and 475–500 ml in *Australopithecus* (electronic supplementary material, table S2). The fact that $\dot{Q}_{ICA}$ is up to twofold higher in *Gorilla* than in *Australopithecus* is surprising, given that the australopithecines have been placed between great apes and humans on the basis of several measures relating to brain and intelligence [23,24]. Apparently, the underlying assumptions that cognitive ability, brain MR and blood flow rate all scale with brain size in parallel, and that the patterns evident in living haplorhine primates apply to hominins, are incorrect. Indeed, this study shows that the scaling of $\dot{Q}_{ICA}$ follows quite different allometries in haplorhines and hominins (figure 2). Chimpanzee and human lineages diverged around 6–7.5 Ma [39,45,46], so it is likely that $\dot{Q}_{ICA}$ was equal or lower than we measure in *Ardipithecus* from 4.4 Ma [47]. From that point, recent chimpanzees ended up higher than *Australopithecus* and modern humans even higher (figure 4). The trajectories of the older lineages of gorillas and orangutans were apparently also rising.

Because the ICAs supply almost all of the cerebrum in humans, we assume that, in addition to increasing brain

size, the rise in volume-specific $\dot{Q}_{ICA}$ in the hominins traces a rapid evolutionary rise in the metabolic intensity of the neural tissue. This would correlate with an increase in cognitive ability from *Australopithecus*, as the early representatives of hominin evolution, to modern *H. sapiens*, that exceeded that determined by brain volume alone. Such development is not inevitable, however, as evidenced by similar values of $\dot{Q}_{ICA}$ and V_{br} in *H. naledi* and *H. floresiensis* to those in *Australopithecus* species, despite approximately 2.5 million years between them [48,49] (figure 4). It is thought that *H. naledi* and *H. floresiensis* branched from ancient small-brained *Homo* ancestors, possibly independently [46,50,51]. These two recent species raise problems in relating cognitive ability to measures of brain perfusion rate as well as brain size [23].

The high cerebral perfusion in recent great apes may relate to living in social family groups [52]. Presumably, a relatively high cognitive capacity is required to interpret family interrelationships and hierarchies and to partake in social behaviours that would render individuals fit for mating and territory defence [53,54]. Such social drivers for cognitive evolution are often attributed to *Australopithecus* and early *Homo*, but could also be ascribed to the great apes that likewise exhibit complex family cooperation. This would have contributed to increases in ancestral great ape cerebral metabolic and ICA blood flow rates, in a similar way to the *Homo* predecessors. It can be argued that the cognitive capacity that favoured the survival of the genus *Homo* equally facilitated the survival of ancestral great apes. The requirement for cerebral specialisation may have ultimately contributed to modern great apes being more cognitively advanced than *Australopithecus*.

4. Methods

New measurements were made from 82 skulls from museum collections that represent all six species of non-human great apes (see electronic supplementary material for specimen data). Endocranial volume (V_{br}; ml) was measured by sealing large foramina in the skull with cotton wool and filling the brain case with rice or plastic beads to the level of the foramen magnum, gently agitating to achieve uniform filling and compaction, and then emptying into a graduated cylinder and recording the compacted volume. Because the carotid artery occupies the foramen lumen almost entirely, the outer radius of the artery is defined by the radius of the foramen (r_o; cm). With recently defined methods [55], the radii of the left and right carotid foramina were measured from photographs, captured orthogonal to the opening, together with a 0.5 mm graduated scale, positioned at the level of the opening. An ellipse was fitted to the inside of the foramen opening with ImageJ (open source, imagej.net), and r_o was taken as the radius of a perfect circle with the measured elliptical area.

The literature was searched for data on lumen radius (r_i, cm) and wall thickness of normally pressurized internal carotid and common carotid arteries. Wall thickness was taken as the difference between outer radius (r_o) and lumen radius (r_i), and was expressed as the ratio $w = (r_o - r_i)/r_i$. The mean value of w was 0.30, which was used in the calculations (see electronic supplementary material, table S1 for data).

Blood flow rate in the ICA was calculated from carotid foramen radius (r_o) by first calculating lumen radius [$r_i = r_o/(1 + w)$] and then applying the new empirical equation ($\dot{Q}_{ICA} = 155 r_i^{2.49}$). The results of this approach are slightly better statistically, but are similar to those from the Poiseuille-derived shear stress equation used previously (see electronic supplementary material for detailed comparison of computational approaches and their results).

The new calculations were applied to r_o and V_{br} data from previous studies of 44 species of extant haplorhine primates [6,13], and 12 species of hominin (two points for early and late *Homo erectus*), including eight specimens attributed to *Australopithecus africanus* and three attributed to *A. afarensis* [43]. A new r_o datum for *Ardipithecus ramidus* was obtained by measuring three scaled figures of the basal skull and taking the mean V_{br} from the publications [44,56]. In addition, $\dot{Q}_{ICA}$ was compared allometrically with the volumes of neocortical grey matter, telencephalon and total neocortex from recent publications [17–19].

Data are presented as means with 95% confidence intervals (CIs). Allometric data were $\log_{10}$-transformed prior to fitting ordinary least-squares linear regressions [57,58] and performing ANCOVA to test for significant differences in scaling exponents and elevations [59]. If the exponents differed significantly, differences in the elevation could not be evaluated, so the Johnson–Neyman technique defined the region in which data from individual species were not significantly different [60]. Statistics on mean data also included ANOVA and Tukey's multiple comparisons test.

Data accessibility. All of the data are in the electronic supplementary material section.

Authors' contributions. R.S.S.: conceptualization; R.S.S., V.B., E.P.S., Q.H., T.J.N., P.C.C., B.Z. and C.V.M.: data gathering; R.S.S., Q.H., V.B. and E.P.S.: formal analysis; R.S.S. and V.B.: writing—original draft; R.S.S., E.P.S., Q.H., T.J.N., P.C.C., B.Z. and C.V.M.: writing—review and editing; R.S.S.: project administration.

Competing interests. We declare we have no competing interests.

Funding. This project 'Design of the cardiovascular system of living and fossil vertebrates' was supported by the Australian Research Council (grant no. DP 170104952).

Acknowledgements. The authors thank John Wible (Carnegie Museum of Natural History), Darrin Lunde (Smithsonian National Museum of Natural History), Brendon Billings (School of Anatomical Sciences, University of the Witwatersrand) and David Stemmer and Catherine Kemper (South Australian Museum) for access to skulls. Permission to measure fossil skulls was generously provided by the Fossil Access Advisory Panel (Evolutionary Studies Institute, University of the Witwatersrand). In particular, Lee Berger and John Hawks gave permission to measure *H. naledi*. Stephany Potze and Lazarus Kgasi graciously allowed access to specimens at the Ditsong National Museum of Natural History, Pretoria. We appreciate the advice of Terrence Ritzman (Washington University of St Louis) about hominin taxonomy and the validity of certain hominin skull casts for measurements of carotid foramen size in our 2016 study. The associate editor and two anonymous referees provided significant advice for revision of the first version of this manuscript.

References

1. Logan CJ *et al*. 2018 Beyond brain size: uncovering the neural correlates of behavioral and cognitive specialization. *Comp. Cogn. Behav. Rev.* **13**, 55–89. (doi:10.3819/ccbr.2018.130008)
2. Deaner RO, Isler K, Burkart J, van Schaik C. 2007 Overall brain size, and not encephalization quotient, best predicts cognitive ability across non-human primates. *Brain Behav. Evol.* **70**, 115–124. (doi:10.1159/000102973)
3. MacLean EL *et al*. 2014 The evolution of self-control. *Proc. Natl Acad. Sci. USA* **111**, E2140–E2148. (doi:10.1073/pnas.1323533111)
4. Karbowski J. 2007 Global and regional brain metabolic scaling and its functional

consequences. *BMC Biol.* **5**, 18. (doi:10.1186/1741-7007-5-18)

5. Karbowski J. 2011 Scaling of brain metabolism and blood flow in relation to capillary and neural scaling. *PLoS ONE* **6**, e26709. (doi:10.1371/journal.pone.0026709)
6. Seymour RS, Angove SE, Snelling EP, Cassey P. 2015 Scaling of cerebral blood perfusion in primates and marsupials. *J. Exp. Biol.* **218**, 2631–2640. (doi:10.1242/jeb.124826)
7. Berlis A, Putz R, Schumacher M. 1992 Direct and CT measurements of canals and foramina of the skull base. *Br. J. Radiol.* **65**, 653–661. (doi:10.1259/0007-1285-65-776-653)
8. Paullus WS, Pait TG, Rhoton AL. 1977 Microsurgical exposure of the petrous portion of the carotid artery. *J. Neurosurg.* **47**, 713–726. (doi:10.3171/jns.1977.47.5.0713)
9. Vijaywargiya M, Deopujari R, Athavale S. 2017 Anatomical study of petrous and cavernous parts of internal carotid artery. *Anat. Cell Biol.* **50**, 163–170. (doi:10.5115/acb.2017.50.3.163)
10. Lehoux S, Tedgui A. 2003 Cellular mechanics and gene expression in blood vessels. *J. Biomech.* **36**, 631–643. (doi:10.1016/S0021-9290(02)00441-4)
11. Boyer DM, Harrington AR. 2018 Scaling of bony canals for encephalic vessels in euarchontans: implications for the role of the vertebral artery and brain metabolism. *J. Hum. Evol.* **114**, 85–101. (doi:10.1016/j.jhevol.2017.09.003)
12. Seymour RS, Snelling EP. 2019 Calculating brain perfusion of primates. *J. Hum. Evol.* **128**, 99–102. (doi:10.1016/j.jhevol.2018.06.001)
13. Boyer DM, Harrington AR. 2019 New estimates of blood flow rates in the vertebral artery of euarchontans and their implications for encephalic blood flow scaling: a response to Seymour and Snelling (2018). *J. Hum. Evol.* **128**, 93–98. (doi:10.1016/j.jhevol.2018.10.002)
14. Seymour RS, Hu Q, Snelling EP, White CR. 2019 Interspecific scaling of blood flow rates and arterial sizes in mammals. *J. Exp. Biol.* **222**, jeb 199554. (doi:10.1242/jeb.199554)
15. Seymour RS, Bosiocic V, Snelling EP. 2017 Correction to 'Fossil skulls reveal that blood flow rate to the brain increased faster than brain volume during human evolution'. *R. Soc. open sci.* **4**, 170846. (doi:10.1098/rsos.170846)
16. Cooper CE, Withers PC. 2006 Numbats and aardwolves—how low is low? A re-affirmation of the need for statistical rigour in evaluating regression predictions. *J. Comp. Physiol. B Biochem. Syst. Environ. Physiol.* **176**, 623–629. (doi:10.1007/s00360-006-0085-8)
17. Navarrete AF, Blezer E.LA, Pagnotta M, de Viet E.SM, Todorov OS, Lindenfors P, Laland KN, Reader SM. 2018 Primate brain anatomy: new volumetric MRI measurements for neuroanatomical studies. *Brain Behav. Evol.* **91**, 109–117. (doi:10.1159/000488136)
18. Stephan H, Frahm H, Baron G. 1981 New and revised data on volumes of brain structures in insectivores and primates. *Folia Primatol.* **35**, 1–29. (doi:10.1159/000155963)
19. Zilles K, Rehkämper G. 1988 The brain, with special reference to the telencephalon. In *Orang-Utan biology* (ed. JH Schwartz), pp. 157–176. Oxford, UK: Oxford University Press.
20. Miller IF, Barton RA, Nunn CL. 2019 Quantitative uniqueness of human brain evolution revealed through phylogenetic comparative analysis. *Elife* **8**, e41250. (doi:10.7554/eLife.41250.001)
21. Barton RA, Venditti C. 2014 Rapid evolution of the cerebellum in humans and other great apes. *Curr. Biol.* **24**, 2440–2444. (doi:10.1016/j.cub.2014.08.056)
22. Schwartz JH, Tattersall I. 1987 Tarsiers, adapids and the integrity of Strepsirhini. *J. Hum. Evol.* **16**, 23–40. (doi:10.1016/0047-2484(87)90059-5)
23. Alba DM. 2010 Cognitive inferences in fossil apes (Primates, Hominoidea): does encephalization reflect intelligence? *J. Anthropol. Sci.* **88**, 11–48.
24. Jerison HJ. 1973 *Evolution of the brain and intelligence*. New York, NY: Academic Press.
25. Seymour RS, Hu Q, Snelling EP. In press. Blood flow rate and wall shear stress in seven major cephalic arteries of humans. *J. Anat.* (doi:10.1111/joa.13119)
26. Zhao XX, Zhao MD, Amin-Hanjani S, Du XJ, Ruland S, Charbel FT. 2015 Wall shear stress in major cerebral arteries as a function of age and gender—a study of 301 healthy volunteers. *J. Neuroimaging* **25**, 403–407. (doi:10.1111/jon.12133)
27. Schöning M, Walter J, Scheel P. 1994 Estimation of cerebral blood flow through color duplex sonography of the carotid and vertebral arteries in healthy adults. *Stroke* **25**, 17–22. (doi:10.1161/01.STR.25.1.17)
28. Scheel P, Ruge C, Schöning M. 2000 Flow velocity and flow volume measurements in the extracranial carotid and vertebral arteries in healthy adults: reference data and the effects of age. *Ultrasound Med. Biol.* **26**, 1261–1266. (doi:10.1016/S0301-5629(00)00293-3)
29. Ford MD, Alperin N, Lee SH, Holdsworth DW, Steinman DA. 2005 Characterization of volumetric flow rate waveforms in the normal internal carotid and vertebral arteries. *Physiol. Meas.* **26**, 477–488. (doi:10.1088/0967-3334/26/4/013)
30. Sato K, Sadamoto T. 2010 Different blood flow responses to dynamic exercise between internal carotid and vertebral arteries in women. *J. Appl. Physiol.* **109**, 864–869. (doi:10.1152/japplphysiol.01359.2009)
31. Wåhlin A, Ambarki K, Hauksson J, Birgander R, Malm J, Eklund A. 2012 Phase contrast MRI quantification of pulsatile volumes of brain arteries, veins, and cerebrospinal fluids compartments: repeatability and physiological interactions. *J. Magn. Reson. Imaging* **35**, 1055–1062. (doi:10.1002/jmri.23527)
32. Zilles K, Palomero-Gallagher N, Amunts K. 2013 Development of cortical folding during evolution and ontogeny. *Trends Neurosci.* **36**, 275–284. (doi:10.1016/j.tins.2013.01.006)
33. Hofman MA. 2014 Evolution of the human brain: when bigger is better. *Front. Neuroanat.* **8**, e00015. (doi:10.3389/fnana.2014.00015)
34. Gregory M, Kippenhan J, Dickinson D, Carrasco J, Mattay V, Weinberger D, Berman K. 2016 Regional variations in brain gyrification are associated with general cognitive ability in humans. *Curr. Biol.* **26**, 1301–1305. (doi:10.1016/j.cub.2016.03.021)
35. Harris JJ, Attwell D. 2012 The energetics of CNS white matter. *J. Neurosci.* **32**, 356–371. (doi:10.1523/JNEUROSCI.3430-11.2012)
36. Harris JJ, Jolivet R, Attwell D. 2012 Synaptic energy use and supply. *Neuron* **75**, 762–777. (doi:10.1016/j.neuron.2012.08.0190)
37. Parkes LM, Rashid W, Chard DT, Tofts PS. 2004 Normal cerebral perfusion measurements using arterial spin labeling: reproducibility, stability, and age and gender effects. *Magn. Reson. Med.* **51**, 736–743. (doi:10.1002/mrm.20023)
38. Wu W-C, Lin S-C, Wang DJ, Chen K-L, Li Y-D. 2013 Measurement of cerebral white matter perfusion using pseudocontinuous arterial spin labeling 3T magnetic resonance imaging—an experimental and theoretical investigation of feasibility. *PLoS ONE* **8**, e82679. (doi:10.1371/journal.pone.0082679)
39. Finstermeier K, Zinner D, Brameier M, Meyer M, Kreuz E, Hofreiter M, Roos C. 2013 A mitogenomic phylogeny of living primates. *PLoS ONE* **8**, e69504.
40. Dicke U, Roth G. 2016 Neuronal factors determining high intelligence. *Phil. Trans. R. Soc. B* **371**, 20150180. (doi:10.1098/rstb.2015.0180)
41. Herculano-Houzel S. 2012 The remarkable, yet not extraordinary, human brain as a scaled-up primate brain and its associated cost. *Proc. Natl Acad. Sci. USA* **109**, 10 661–10 668. (doi:10.1073/pnas.1201895109)
42. Bauernfeind AL *et al*. 2013 A volumetric comparison of the insular cortex and its subregions in primates. *J. Hum. Evol.* **64**, 263–279. (doi:10.1016/j.jhevol.2012.12.003)
43. Seymour RS, Bosiocic V, Snelling EP. 2016 Fossil skulls reveal that blood flow rate to the brain increased faster than brain volume during human evolution. *R. Soc. open sci.* **3**, e160305. (doi:10.1098/rsos.160305)
44. Suwa G, Asfaw B, Kono RT, Kubo D, Lovejoy CO, White TD. 2009 The *Ardipithecus ramidus* skull and its implications for hominid origins. *Science* **326**, 68. (doi:10.1126/science.1175825)
45. Glazko GV, Nei M. 2003 Estimation of divergence times for major lineages of primate species. *Mol. Biol. Evol.* **20**, 424–434. (doi:10.1093/molbev/msg050)
46. Dembo M, Matzke NJ, Mooers AO, Collard M. 2015 Bayesian analysis of a morphological supermatrix sheds light on controversial fossil hominin relationships. *Proc. R. Soc. B* **282**, 133–141. (doi:10.1098/rspb.2015.0943)
47. Lovejoy CO, Suwa G, Simpson SW, Matternes JH, White TD. 2009 The Great Divides: *Ardipithecus ramidus* reveals the postcrania of our last common ancestors with African apes. *Science* **326**, 100–106. (doi:10.1126/science.1175833)
48. Dirks PHGM *et al*. 2017 The age of *Homo naledi* and associated sediments in the Rising Star Cave, South Africa. *Elife* **6**, e24231. (doi:10.7554/eLife.24231.001)

49. Sutikna T *et al*. 2016 Revised stratigraphy and chronology for *Homo floresiensis* at Liang Bua in Indonesia. *Nature* **532**, 366–369. (doi:10.1038/nature17179)
50. Holloway RL, Hurst SD, Garvin HM, Schoenemann PT, Vanti WB, Berger LR, Hawks J. 2018 Endocast morphology of *Homo naledi* from the Dinaledi Chamber, South Africa. *Proc. Natl Acad. Sci. USA* **115**, 5738–5743. (doi:10.1073/pnas.1720842115)
51. Argue D, Groves CP, Lee MSY, Jungers WL. 2017 The affinities of *Homo floresiensis* based on phylogenetic analyses of cranial, dental, and postcranial characters. *J. Hum. Evol.* **107**, 107–133. (doi:10.1016/j.jhevol.2017.02.006)
52. Imanishi K. 1960 Social-organization of subhuman primates in their natural habitat. *Curr. Anthropol.* **1**, 393–407. (doi:10.1086/200134)
53. Clutton-Brock TH. 1974 Primate social organisation and ecology. *Nature* **250**, 539–542. (doi:10.1038/250539a0)
54. Pawłowski B, Lowen CB, Dunbar RIM. 1998 Neocortex size, social skills and mating success in primates. *Behaviour* **135**, 357–368. (doi:10.1163/156853998793066285)
55. Hu Q, Nelson TJ, Seymour RS. In press. Bone foramen dimensions and blood flow calculation: best practices. *J. Anat.* (doi:10.1111/joa.13106)
56. Kimbel WH, Suwa G, Asfaw B, Rak Y, White TD. 2014 *Ardipithecus ramidus* and the evolution of the human cranial base. *Proc. Natl Acad. Sci. USA* **111**, 948–953. (doi:10.1073/pnas.1322639111)
57. Kilmer JT, Rodríguez RL. 2016 Ordinary least squares regression is indicated for studies of allometry. *J. Evol. Biol.* **30**, 4–12. (doi:10.1111/jeb.12986)
58. Smith RJ. 2009 Use and misuse of the reduced major axis for line-fitting. *Am. J. Phys. Anthropol.* **140**, 476–486. (doi:10.1002/ajpa.21090)
59. Zar JH. 1998 *Biostatistical analysis*. Upper Saddle River, NJ: Prentice Hall.
60. White CR. 2003 Allometric analysis beyond heterogeneous regression slopes: use of the Johnson-Neyman technique in comparative biology. *Physiol. Biochem. Zool.* **76**, 135–140. (doi:10.1086/367939)